

S. Fares<sup>1</sup>, A. Ashour<sup>1</sup>, M. El-Ashry<sup>2</sup>  
and M. Abd El-Rahma<sup>1</sup>

<sup>1</sup> Department of Radiation Physics, National Center of Radiation Research and Technology NCRRT, Atomic Energy Authority, Cairo, Egypt

<sup>2</sup> Physics Department, Faculty of Science, Suez Canal University, Ismailia 41522, Egypt

## Gamma Radiation Hazards and Risks Associated with Wastes from Granite Rock Cutting and Polishing Industries in Egypt

*Geological materials usually contaminated with naturally occurring radioactive materials (NORM) have become a focus of great attention. The gamma radiation in samples of a variety of natural tiling rocks (granites) collected from different factories in Egypt for use in the building industry was measured, employing high-resolution g-ray spectrometry.*

*In order to assess the radiological impact from the granites investigated. The radiological hazard indices, annual effective dose equivalent (outdoor and indoor) ( $D_{eff}$ ), hazard indices ( $H_{ex}$  and  $H_{in}$ ), activity utilization indices ( $Ig, Ia$ ) and excess life time cancer risk (ELCR) were calculated. The radiological hazard indices for most granite samples are higher than the internationally recommended values.*

*Keywords: gamma ray spectrometry; NORM; Radiological risk; Natural radioactivity; Activity concentration of  $^{238}U$ ,  $^{226}Ra$ ,  $^{232}Th$  and  $^{40}K$ ; Absorbed dose rate; Annual effective dose rate; Tiling rocks (granites); Activity utilization index; Granite Waste materials; Energy dispersive X-ray spectrometry (EDS), XRD.*

**С. Фаре, А. Ашур, М. Ель-Ешрі, М. Абд Ель-Рахман**

**Небезпека гамма-випромінювання та ризики, пов'язані з промисловими операціями з різання й шліфування граніту в Єгипті**

*Із застосуванням гамма-спектрометрії високого розділення виміряна потужність гамма-випромінювання зразків різних природних облицювальних порід (гранітів), відібраних на різних підприємствах Єгипту і використовуваних у будівельній промисловості.*

*Виконано дослідження й аналіз фізичних і хімічних характеристик зразків граніту для встановлення їх взаємозв'язку з вмістом радіонуклідів.*

*Ключові слова: гамма-спектрометрія; природна радіоактивність, облицювальні породи (граніти), коефіцієнт використання активності.*

© S. Fares, A. Ashour, M. El-Ashry and M. Abd El-Rahma, 2012

Natural radiation refers to ionizing radiation originating either from high energy cosmic rays entering the earth's atmosphere from outer space or from naturally occurring radioactive materials (NORM) present in the crust of the earth. This radiation is distinguished from artificial radiation produced through man-made nuclear or atomic transformations. The exposure of human beings to a background of natural radiation is a continuing and inescapable feature of life on earth. The effective dose due to this ionizing radiation for members of the public varies substantially depending on where they live, occupation, personal habits, diet, building type and house utilization pattern [1]. Higher radiation levels are associated with igneous rocks, such as granite, and lower levels are associated with sedimentary rocks. There are exceptions, however, as some shale and phosphate rocks have a relatively high content of radionuclides [2]. When radioactive material in rocks disintegrates through natural processes, radionuclides are carried to soil by rain and flows [3]. In addition to the natural sources; soil radioactivity is also affected by man-made activities.

The petrologic features of granitic rock associated with a common major minerals contain very low U and Th contents. Both occur primarily in certain accessory minerals (minute inclusions in major minerals) in which they are either major constituents or replace other elements [4,5]. The list of these includes oxides (uraninite, thorinite), silicates (zircon, thorite, allanite), phosphates (monazite, apatite, xenotime) and titanosilicates (titanite minerals) [6,7]. The potassium content of rocks also increases with acidity. Potassium is usually found in potash feldspars, such as microcline and orthoclase, or in micas, like muscovite and biotite. Rocks that are free of these minerals have very low K-activity. The background levels in rocks from the  $^{238}U$  and  $^{232}Th$  series and from  $^{40}K$  make similar contributions to the externally incident gamma radiation where the median concentrations of  $^{238}U$ ,  $^{232}Th$  and  $^{40}K$  in the earths crust lie from outer space around 35, 30 and 400 Bq/kg respectively [8]. Secular equilibrium in the decay series (where activities of all daughter nuclides are equal to the activity of their respective parents) is rarely achieved in most surface and near-surface geological environments, because nuclides of the chains are subject to migration due to physical or chemical processes [9]. Quantification of background levels of radio nuclides is necessary to evaluate the potential environmental risk, to determine the boundary of a contaminated area and to establish its clean up level [10]. In terms of natural radioactivity, granites exhibit an enhanced elemental concentration of uranium (U) and thorium (Th) compared to the very low abundance of these elements observed in the mantle and the crust of the Earth. Geologists provide an explanation of this behavior in the course of partial melting and fractional crystallization of magma, which enables U and Th to be concentrated in the liquid phase and become incorporated into the more silica-rich products. For that reason, igneous rocks of granitic composition are strongly enriched in U and Th (on an average of 5 ppm of U and 15 ppm of Th), compared to rocks of basaltic or ultramafic composition (< 1 ppm of U) [6,11].

Distinct types of granites have different geological origins and mineralogical compositions and may be either magmatic or metamorphic rocks [12]. Concerning their compositions, granites are mixtures of minerals of visible multicolored grains. One colour grains are typically encircled by grains of other colors, e.g. gray quartz is close to pink orthoclase, white plagioclase and dark mica. Every commercial granite contains feldspar (hardness 6 in Mohs Scale) of various colours: white, pink, red,

yellow, brown, green and gray. Feldspar grains are typically not translucent and have a cleavage. Many granites, especially of light colors, contain quartz (hardness 7 in Mohs Scale) with gray (sometimes bluish) colour and the grains are glassy translucent without cleavage. Further, there are dark minerals such as hornblende, pyroxene and biotite with black, dark green or dark brown colours. These minerals have larger specific gravity and lower hardness than feldspars and quartz. Granites, usually suitable as building and ornamental materials [13] for interior and exterior use, are hard natural stones that require harder tools to be cut, shaped and polished.

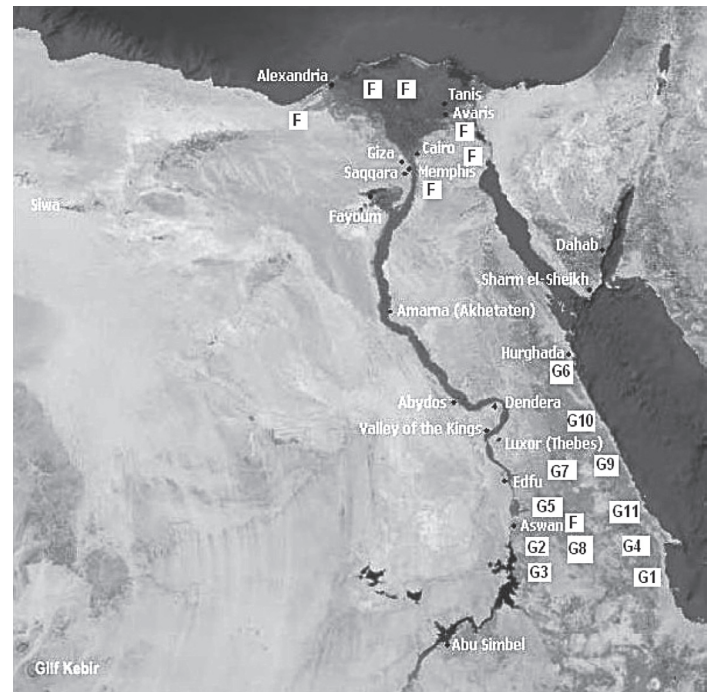
Characterization of dismantled items with very low radioactivity levels and intended for recycling or reuse can be an extremely complex and expensive operation if their radiological characteristics are unknown. In such circumstances, numerous additional measurement and analysis methods must be implemented to determine the activity of each radionuclide liable to be present in or on the material. In order to optimize the means required for characterization, it is essential to determine beforehand the most possible accurate data on the nature, composition, distribution and order of magnitude of the actual radioactivity. Recycling of material is in most cases a more “environmental friendly” option than producing new material. Reuse of facilities is also advisable in most situations. This calls for setting regulatory limits for recycling and reuse at levels that balance the advantage of recycling and the risk (including the radiation risk) of using the recycled material. All building raw materials and products, including granite, derived from rock and soil contain various amounts of mainly natural radionuclides of the uranium  $^{238}\text{U}$  and thorium  $^{232}\text{Th}$  series, and the radioactive isotope of potassium  $^{40}\text{K}$ . In the  $^{238}\text{U}$  series, the decay chain segment starting from radium  $^{226}\text{Ra}$  is radiologically the most important and, therefore, reference is often made to  $^{226}\text{Ra}$  instead of  $^{238}\text{U}$ . These radionuclides are sources of the external and the internal radiation exposures in dwellings. It is a common practice to use industrial by-products and recycle certain industrial residues and waste as raw materials for the building industry. Concern for potential risks arises where the residues used as raw materials for building products are derived from NORM contaminated waste materials. In order to assess the radiological hazards to human health, it is important to study the radioactivity levels emitted by these materials. This paper is dealing with the natural radioactivity in association with the mineralogical and chemical features of granites used as building materials in order to understand the relationship between natural radioactivity and the radioactive minerals present. We also carried out an assessment of dose exposure based on activities of studied granites. The data obtained from that study are essential for development of standards and guidelines concerning the use and management of granite as a building materials.

## 1. Experimental methods

### 1.1. Sample collection and preparation

Samples of 11 different types of the main Egyptian commercial granites were collected directly from the producers in ten Egyptian State as shown in Fig. 1. We did so in order to avoid eventual miss identifications of the granites, due to the fact that in the stone markets there are examples in which different granites are sold as if they had the same commercial name or in other words, the same granite has different names.

Similarly it happens in the extraction zone that, some-times, blocks of granites showing small heterogeneities due to the distribution of multicolored grains, are extracted from the same mining area (in some cases, from the same rock out-cropping) are classified with different commercial names, although their basic mineralogical composition had not been changed. Thus, all of these collected granite samples were classified in accordance to their colors, sites of extraction and mineralogical compositions.



G- GRANITE  
F- FACTORIES

Fig. 1. Map of the Sampling Sites and Factories in Egypt

The samples were dried in an oven at  $110\text{ }^{\circ}\text{C}$  till constant dry weight was obtained, crushed and homogenized. The homogenized samples were packed in a 250 ml plastic container to its full volume with uniform mass. These containers were shielded hermetically and externally to ensure that all daughter products of uranium and thorium, in particular, radon gas formed, do not escape. The net weight of the sample was determined before counting. These samples were then stored for 30–40 days before counting so as to ensure  $^{226}\text{Ra}$  and its short-lived progeny to reach radioactive equilibrium [14–17].

### 1.2. Radioactivity Measurements

The activity concentration of the natural radioactivity  $^{238}\text{U}$ ,  $^{226}\text{Ra}$ ,  $^{232}\text{Th}$  and  $^{40}\text{K}$  in the samples were determined using a high-resolution HPGe g-spectrometry system with 30% counting efficiency. The resolution of this spectrometer was 1.89 keV at 1332 keV g-rays of  $^{60}\text{Co}$ . The efficiency calibration of the gamma-ray spectrometer was performed with the radionuclide specific efficiency method in order to avoid any uncertainty in gamma-ray intensities as well as the influence of coincidence summation and self-absorption effects of the emitting gamma photons. A set of high quality certified reference materials (IAEA, RG-set) was used, with densities similar to the building

materials measured after pulverization. This was performed by taking 250 cm<sup>3</sup> counting vials filled up to a height of 7 cm, which correspond to 170 cm<sup>3</sup>, with reference building materials. The measurement duration was up to 80 000 sec and were carried out in the Laboratory of Atomic and Nuclear Physics, Department of Physics, Suez Canal University.

The obtained spectra were analyzed with the use of Canberra Genie 2000 software version 3.0. The determination of the presence of radionuclides and calculation of their activities were based on the following gamma-ray transitions (in keV): the <sup>226</sup>Ra activities (or <sup>238</sup>U activities for samples assumed to be in radioactive equilibrium) were estimated from <sup>234</sup>Th (92.38 keV, 5.6 %), while g-energies of <sup>214</sup>Pb (351.9 keV, 35.8 %) and <sup>214</sup>Bi (609.3, 45 %), (1764.5 keV, 17 %) and <sup>226</sup>Ra (185.99 KeV, 3.5 %) were used to estimate the concentration of <sup>226</sup>Ra. The gamma-ray energies of <sup>212</sup>Pb (238.6 keV, 45 %), and <sup>228</sup>Ac (338.4 keV, 12.3 %), (911.07 keV, 29 %), (968.90 keV, 17 %) were used to estimate the concentration of <sup>232</sup>Th. The natural abundance of <sup>235</sup>U is only 0.72 % of the total uranium content and hence was not considered in the present study. The activity concentrations of <sup>40</sup>K were measured directly by its own gamma rays (1460.8 keV, 10.7 %).

In order to determine the background distribution due to naturally occurring radionuclides in the environment around the detector, an empty polystyrene container was counted in the same manner as the samples. The activity concentrations were calculated after measurement and subtraction of the background. The activities were determined from measuring their respective decay daughters [18]. The activity concentrations were calculated from the intensity of each line taking into account the mass of the sample, the branching ratios of the g-decay, the time of counting and the efficiencies of the detector [19,20]. The activity concentrations of the investigated samples were calculated from equation (1):

$$A = (\text{CSP})_{\text{net}} / I \times E_{\text{ff}} \times M, \quad (1)$$

where A is the activity concentration in Bq/kg, (cps)net is the (count per second) and equal {(cps)sample/(cps)B.g}, I is the intensity of the  $\gamma$ -line in a radionuclide,  $E_{\text{ff}}$  is the measured efficiency for each  $\gamma$ -line observed and M is the mass of the sample in kilograms.

The correction for the contribution of <sup>232</sup>Th via its daughter nuclide <sup>228</sup>Ac (1459.2 keV peak) to the 1460.8 keV peak of <sup>40</sup>K was made according to [21]:

$$\text{The error in } ^{40}\text{K activity (\%)} = 9.3(A_{\text{Th}}/A_{\text{K}}), \quad (2)$$

where  $A_{\text{Th}}$  and  $A_{\text{K}}$  are the activity concentration of <sup>232</sup>Th and <sup>40</sup>K, respectively, in Bq·kg<sup>-1</sup>.

### 1.3. Mineralogical Measurements

Compositions Assessment using EDEX Technique. Energy-dispersive X-ray spectroscopy, (EDS or EDX) is an analytical technique used for the elemental analysis or chemical characterization of a sample. It is one of the variants of X-ray fluorescence spectroscopy analyzing X-rays emitted by the matter in response to being hit with charged particles, e.g. in SEM the sample is subjected to an energetic electron beam (20 keV) resulting in production of characteristic X-rays from the sample. The number and energy of the X-rays emitted from a specimen can be measured by an energy-dispersive spectrometer. As the

energy of the X-rays is characteristic of the difference in energy between the two shells, and of the atomic structure of the element from which they were emitted, this allows the elemental composition of the specimen to be measured. The samples were grounded to an as fine particle size as possible in a laboratory mill. The resulting powder was pressed into pellets of 40 mm diameter and 5 mm thickness. The main mineralogical composition of the granite samples were determined from the XRD analysis using a powdered X-ray diffractometer (model XD-DI, Shimadzu, Japan) equipped with a copper target and nickel filter.

## 2. Results and discussion

### 2.1. Elemental analysis

Chemical composition of samples shows in Table 1 which forgets by using analysis (EDEX). It can be observed that in all of them, Si is the predominant, followed by Al and other elements such as Mg, Na, S, Ti, Zn, Cu, K, Cl and Fe are also present. Since the majority of the examined samples have granitic composition, the K concentration of the rocks is expected to be generally high. Indeed, only G(7) and G(9) samples, having gabbroic and monzodioritic (basic) composition, respectively. Based on that G(9) shows <sup>40</sup>K activity concentrations lower than that of the regular soil in contrast to the rest samples showing values as high as two to four times the regular soil <sup>40</sup>K activity concentration Table 2.

Another interesting point is that the red colored granite samples, i.e. G(1,2, 5,6) Table 1, are highly radioactive. The red color of feldspars is due to hematite inclusions [22]. According to [23], hematite could be radioactive containing uranium. Thus, it is possible that hematite inclusions in feldspars might contribute insignificantly to the level of natural radioactivity of G(4), G(5), and G(6) red granites. However, no data are available to support this suggestion. Although G (7) presents a significant amount of iron, it has been expressed in terms of Fe (14.24 wt.%), activity index ( $I_g = 1.87$ ) relatively low compared to other samples which can be interpreted as, some iron consists of fine, abrasive shoot particles used in the granite cutting operation. Iron oxide is an auxiliary fluxing agent and is responsible for the reddish color of sintered products. The significant amount of iron is responsible for a darker coloring of the sintered samples. As for the other highly radioactive samples, one of them was light gray G(11), one was white G(10) and one was pink G(4).

The granite samples reject are formed basically by SiO<sub>2</sub>, Al<sub>2</sub>O<sub>3</sub>, Fe<sub>2</sub>O<sub>3</sub>, K<sub>2</sub>O and CaO, with small amounts of MgO, CuO, SO<sub>3</sub>, ZnO and Na<sub>2</sub>O [24]. As it was pointed out, Table 1, K-rich minerals (K- feldspars and biotite) are main rock-forming mineral constituents of almost all the rocks. Hence, the K-rich minerals contribute to the level of the natural radioactivity of the samples investigated. Among the accessory minerals of the samples, the ones containing uranium or thorium, and hence considered as radioactive [23], are shown in Table 1 along with the activity index ( $I_g$ ). Such high indices suggest a potential high external dose rates associated with these significant naturally occurring radio nuclides.

X-ray diffraction technique has been used to investigate the structure and characteristics of the prepared samples. The obtained x- ray diffraction patterns of the investigated powder samples are shown in figure 2. The XRD analysis showed three main peaks characteristic of calcium and silicate minerals,



Table 1: Chemical Composition of Granite Samples ( wt.%)

Sample	Region	Commercial name Element	Na	Al	Si	S	Cl	K0	Ca	Mn	Fe	Cu	Zn	I <sub>γ</sub>
G(1)	Halyb&Chalteen	Halyb&Chalteen	8.73	12.55	56.45	0.15	0.20	7.40	2.73	0.45	9.89	0.84	0.87	2.46
G(2)	Aswan	RedKamek	2.67	9.98	67.20	0.29	0.51	8.10	3.18	0.16	6.35	0.76	0.80	2.22
G(3)	Aswan	GreenFardey	4.29	10.39	68.01	0.34	0.28	6.3	5.37	-	2.22	1.30	1.36	2.13
G(4)	Aswan	RozaHodey	8.63	13.10	60.36	0.20	0.27	8.84	1.62	0.20	6.60	0.15	0.03	2.93
G(5)	Aswan	GandoulaRed	2.83	10.29	65.91	0.23	0.13	7.60	7.01	0.07	4.25	0.84	0.83	3.25
G(6)	RedSea	BrownElqusar	0.87	9.62	68.32	0.28	0.29	9.42	4.63	0.09	4.15	1.16	1.17	3.24
G(7)	Aswan	Gandoul	-	10.12	59.64	0.21	0.23	4.61	12.14	0.35	14.24	0.39	0.42	1.87
G(8)	Aswan	RamadyAswan	3.70	9.78	67.43	0.24	0.32	8.74	4.53	0.05	3.13	1.07	1.00	2.06
G(9)	Aswan	Black	2.54	7.90	73.86	0.32	0.17	2.6	5.67	-	4.90	1.43	0.79	1.41
G(10)	Aswan	Royal	6.80	14.52	56.77	0.08	0.24	11.01	5.55	0.22	2.99	0.86	0.96	2.71
G(11)	Aswan	Fray	1.69	10.54	66.15	-	-	8.33	4.29	0.23	6.27	0.99	1.65	2.09

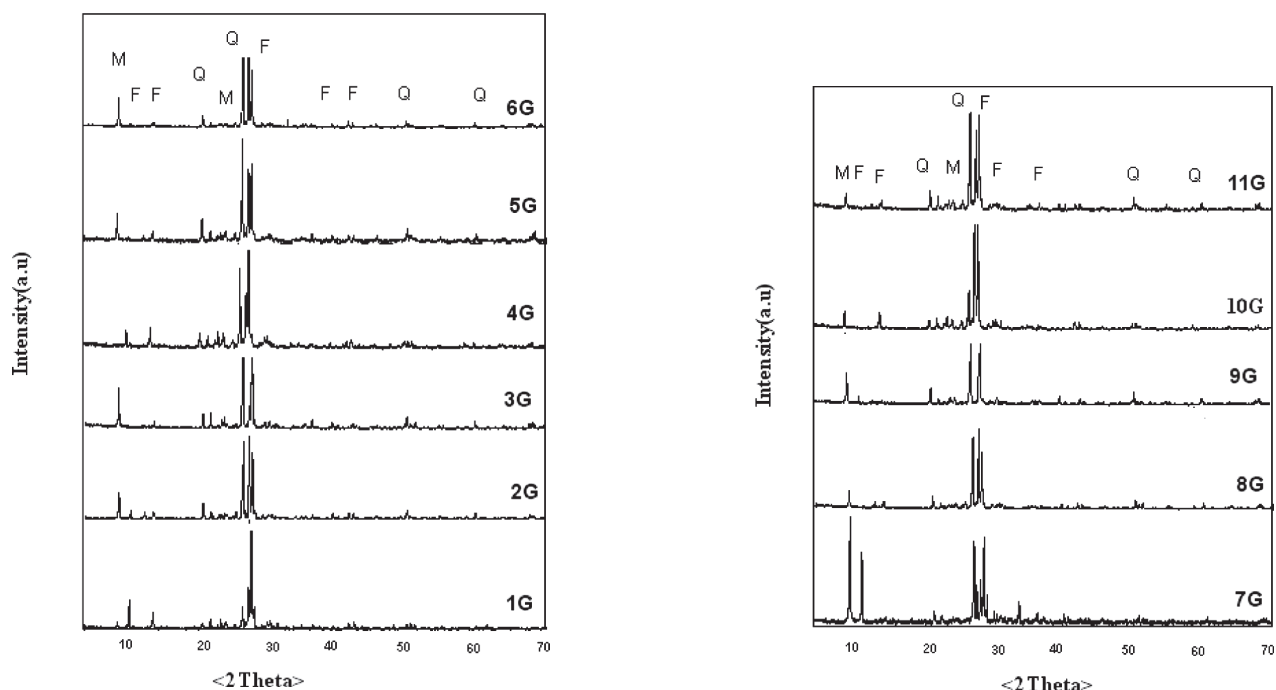


Fig. 2. XRD Patterns of Granite Samples (Q: quartz, M: mica, F: feldspars)

while other minor phases are attributed to metallic impurities. This figure reveals that for Table 1 there is diffraction peaks; the samples are found in the crystalline states.

Fig. 2 shows the XRD patterns of the granite samples. These diffraction patterns indicate that the presence of a micaceous mineral, amphibole, quartz, plagioclase (calcium-sodium feldspar) and potash feldspar can be observed in the granite samples. Both the micaceous mineral and feldspar are the sources of  $K_2O$  and  $Na_2O$ . In the granite waste, the presence of quartz, mica, plagioclases and microcline was observed. The results from Fig. 2 show that the silica is major in different samples ( $\theta \approx 27$ ).

## 2.2. Activity Concentration Analysis (A)

The activity concentrations vary from site to site, which means a large variation in chemical and mineralogical properties [24]. In all sampling sites, activity concentrations are in order  $^{232}Th < ^{238}U < ^{40}K$ . In particular G(4), G(5) and G(6), the activity concentrations of  $^{238}U$  is high, which could be due to the solubility and mobility of  $U(VI)O_2^{2+}$  [25]. Increasing concentrations of  $^{232}Th$  and  $^{40}K$  may be due to the high content of monazite [26]. However in some sites the concentration of  $^{232}Th$  is higher than world average value, indicating that monazite may exist at that site.

Table 2. Activity Concentration for Different Egyptian Granite Samples of U, Ra, Th and K in (Bq | Kg), for (U, Th) in (PPm), (K) in (%) and Clark Values (Ratio of Th to U). Uncertainties are Given Within One Standard Deviation.

Th/U	$A_K(\%)$	$A_{Th}(\text{ppm})$	$A_U(\text{ppm})$	$A_K (\text{Bq/Kg})$	$A_{Th}(\text{Bq/Kg})$	$A_{Ra}(\text{Bq/Kg})$	$A_U(\text{Bq/Kg})$	Sample
0.16	3.26±0.04	8.80±0.71	18.35±1.04	1034.76±12.2	35.63±2.8	212.71±13.9	228.42±13.0	G(1)
0.23	3.70±0.06	8.05±0.48	11.59±0.83	1172.04±19.9	32.58±1.9	167.67±19.6	144.34±10.3	G(2)
0.22	2.63±0.05	6.75±1.0	10.13±0.81	834.16±16.7	27.33±4.0	194.44±17.9	126.10±10.1	G(3)
0.20	3.94±0.07	12.18±1.18	19.81±1.62	1248.64±20.9	49.33±4.7	240.78±21.4	246.58±20.2	G(4)
0.29	3.61±0.06	18.70±1.28	21.08±1.66	1144.64±19.0	75.71±5.1	258.96±22.2	262.40±20.7	G(5)
0.20	3.95±0.07	15.47±1.17	25.47±1.73	1254.80±21.1	62.64±4.7	267.20±29.8	317.02±21.6	G(6)
0.17	1.94±0.05	6.76±0.98	12.65±1.38	615.92±14.4	27.36±3.9	178.45±17.7	157.42±17.2	G(7)
0.20	3.94±0.07	5.49±1.2	9.11±0.87	1250.16±22.6	22.24±4.8	150.83±19.1	113.46±10.8	G(8)
0.09	1.11±0.04	2.47±0.77	9.33±0.68	353.08±11.6	10.00±3.1	161.40±15.6	116.16±8.5	G(9)
0.26	4.61±0.07	10.69±1.13	13.31±0.93	1462.00±22.3	43.26±4.5	194.76±20.5	165.68±11.6	G(10)
0.11	3.78±0.06	3.52±0.53	9.97±0.76	1197.52±19.8	14.26±2.1	172.49±16.7	124.16±9.4	G(11)
0.19	3.32±0.06	8.99±0.95	14.62±1.1	1051.61±18.2	36.39±3.8	199.97±19.5	181.98±13.9	Average

The activity concentrations (Bq/kg) of  $^{238}\text{U}$ ,  $^{226}\text{Ra}$ ,  $^{232}\text{Th}$  and  $^{40}\text{K}$  along with the average values for the 11 granite examined samples collected from suppliers, grinding plants and factories in Egypt are presented in Table 2, where it is clear that the concentrations of  $^{238}\text{U}$  and  $^{226}\text{Ra}$  are higher than that of  $^{232}\text{Th}$ . The concentration of  $^{238}\text{U}$  ranged from 113.46 to 317.02 (Bq/kg) and The concentration of  $^{226}\text{Ra}$  ranges from 150.83 to 267.20 (Bq/kg) while the concentration of  $^{232}\text{Th}$  ranges from 10.00 to 75.71 (Bq/kg). The uranium concentration increases until it reaches its maximum value at locations G(6) and G(5) then it begins to decrease. The obtained results for  $^{238}\text{U}$  for all samples are higher than the permissible levels [27] of (35, 35,30 and 370) Bq/kg. Concerning  $^{40}\text{K}$  the activity concentrations are high in all locations except G(9) location. Regarding  $^{232}\text{Th}$ , five of the samples G(3,7,8,9,11) show activity concentrations lower than the regular soil (lower than the minimum detectable activity up to 30 Bq kg<sup>-1</sup>). Sample G(6) show activity concentration value higher than the double of the regular soil 62.64 Bq kg<sup>-1</sup> value. Since the majority of the examined samples have granitic composition the  $^{40}\text{K}$  activity concentration of the rocks is expected to be generally high. Indeed, only G(9), having gabbroic and monzodioritic (basic) composition, show lower  $^{40}\text{K}$  activity concentrations than these of the regular soil. The rest samples showing values as high as two to four times the regular soil of  $^{40}\text{K}$  activity concentration Table 2.

Table 2 presents also the activity concentration of  $^{238}\text{U}$ , and  $^{232}\text{Th}$  as well as  $^{40}\text{K}$  (Bq/kg) were converted to concentrations of  $^{238}\text{U}$  and  $^{232}\text{Th}$  in (ppm) as well as  $^{40}\text{K}$  in % using the conversion factors given by [28], showing that they range from 9.11 to 25.47 (ppm), from 2.47 to 18.70 (ppm), and from 1.11 to 4.61(%) respectively. Since Th and U elements are considered because of radioactive toxicity, it is important to check if they are above the international levels or not. Permissible concentra-

tions of Th and U in the building materials should not exceed the internationally accepted levels of 20 and 10 mg/kg, respectively [29]. The mean obtained values for U are not within the international accepted values in general. It is also clear that the ratio  $^{232}\text{Th}/^{238}\text{U}$  is less than 3.5 (Clark's value), which denotes enrichment of uranium in the area under investigation. The activity concentrations of  $^{238}\text{U}$ ,  $^{226}\text{Ra}$ ,  $^{232}\text{Th}$  and  $^{40}\text{K}$  of the examined samples are compared as shown in Fig. 3.

Fig.3. Histogram Comparing The Activity Concentration For U,Ra,Th and K in The Granite Samples.

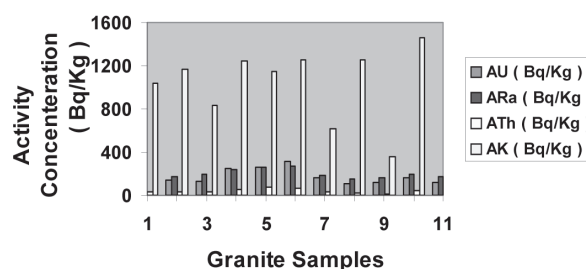


Fig. 3. Histogram comparing the activity concentration for U, Ra, Th and K in the Granite samples

The average activity concentrations of the natural radionuclides of granites from different countries all over the world are shown in Table 3 for comparison, was reported by [30]. It is clear that the average activity concentrations of  $^{238}\text{U}$ ,  $^{226}\text{Ra}$ ,  $^{232}\text{Th}$  and  $^{40}\text{K}$  of the samples in the present study are slightly higher (181.98, 199.97, 36.39 and 1051.61 Bq kg<sup>-1</sup>, respectively) than those reported by [30] for granites from different countries all over the world (42, 73 and 1055 Bq kg<sup>-1</sup>, respectively).

Table 3. Comparison of Radionuclide Concentrations (Bq kg<sup>-1</sup>) in Granite Samples with those Obtained in other Published Data, (The Average Activity Concentrations for Regular Soil are also Shown)

References	A <sub>u</sub> (Bq/Kg)	A <sub>Ra</sub> (Bq/Kg)	A <sub>Th</sub> (Bq/Kg)	A <sub>k</sub> (Bq/Kg)	Country	Location
Chen and Lin (1996) [30]	42	42	73	1055	Average from different countries all over the world	Chen and Lin (1996)
UNSCEAR (2000) [27]	35	35	30	400	-	Regular soile (global scale)
Tzortzis et al. (2003) [4]		1–588	1–906	50–1606	Cyprus	Cyprus
El-Arabi (2005) [31]	-	10–90	98–160	73–102	Egypt	W.Allaki
Anjos et al. (2004) [32]	-	43–651	51–351	418–1618	Turkey	Turkey
Orgun et al. (2005) [26]	-	31	73	1648	Brazil	Brazil
Ahmed et al. (2006) [33]		25–59	28–759	970–1280	Egypt	Wadi El-Gemal
S.Fares et al.	181.98	199.97	36.39	1051.61	Egypt	Present work

This comparison was indicate that the variations in activity concentrations of radium isotopes content in NORM samples of different origins could be due to geological considerations.

### 2.3. Calculation of Radiological Effects

#### 2.3.1. Absorbed Gamma Dose Rate (D)

In order to assess the radiological impact of granites used as building materials. In the UNSCEAR and the European Commissions reports, the dose conversion coefficients were calcu-

lated for the standard room model of a rectangular parallelepiped on house building 3m x 3m x 3m, with infinite thin walls without doors and windows was of dimensions commonly considered [2].

The g-radiation doses are due to the sample content of radionuclides which can be estimated by employing the convenient formula [34]:

$$D = (0.621A_{Th} + 0.462A_{Ra} + 0.0417A_K) \text{ nGyh}^{-1}, \quad (3)$$

where A<sub>Th</sub>, A<sub>Ra</sub> and A<sub>K</sub> represent the activity concentrations of <sup>232</sup>Th, <sup>226</sup>Ra and <sup>40</sup>K in Bqkg<sup>-1</sup> respectively, The ab-

Table 4. Absorbed Dose Rate D (nGy h<sup>-1</sup>), Annual Effective Dose Rate D<sub>eff</sub> (mSv y<sup>-1</sup>) and the Internal and External Hazard Indices for Different Granite Samples

H <sub>ex</sub>	H <sub>in</sub>	D <sub>eff</sub> (indoor) (mSv/y)	D <sub>eff</sub> (outdoor) (mSv/y)	D (nGy/h)	Sample
0.93±0.05	1.50±0.08	0.84±0.05	0.21±0.012	170.81±10.4	G(1)
0.82±0.04	1.28±0.07	0.67±0.07	0.17±0.017	135.79±13.9	G(2)
0.80±0.05	1.33±0.07	0.54±0.07	0.13±0.015	110.01±13.6	G(3)
1.10±0.08	1.75±0.13	0.96±0.08	0.24±0.020	196.62±16.3	G(4)
1.23±0.08	1.93±0.14	1.06±0.08	0.26±0.021	215.98±16.9	G(5)
1.22±0.08	1.95±0.14	1.17±0.08	0.29±0.020	237.69±16.5	G(6)
0.72±0.06	1.20±0.11	0.57±0.06	0.14±0.016	115.40±13.4	G(7)
0.75±0.05	1.16±0.08	0.58±0.07	0.15±0.019	118.36±15.0	G(8)
0.55±0.04	0.98±0.06	0.37±0.06	0.09±0.014	74.60±11.6	G(9)
1.00±0.05	1.52±0.09	0.81±0.08	0.20±0.018	164.37±15.7	G(10)
0.77±0.04	1.24±0.06	0.57±0.06	0.14±0.015	116.15±12.2	G(11)
0.90±0.06	1.44±0.09	0.74±0.07	0.18±0.017	150.53±14.1	Average

sorbed gamma dose rates in air 1m above the ground surface for the uniform distribution of radionuclides ( $^{232}\text{Th}$ ,  $^{238}\text{U}$ , and  $^{40}\text{K}$ ) were computed on the basis of guidelines provided by UNSCEAR [1993, 2000] [2, 27]. The conversion factors used to compute absorbed gamma dose rates (D) in air per unit activity concentration in (Bq/kg) samples are  $0.621 \text{ nGyh}^{-1}$  for  $^{232}\text{Th}$ ,  $0.462 \text{ nGyh}^{-1}$  for  $^{238}\text{U}$ , and  $0.0417 \text{ nGyh}^{-1}$  for  $^{40}\text{K}$  [35-37]. The recommended acceptable total absorbed dose rate by the workers in areas containing g-radiations from  $^{238}\text{U}$  and  $^{232}\text{Th}$  series and their respective decay progenies, as well as  $^{40}\text{K}$ , must not exceed  $55 \text{ nGy/h}$  [2]. It is obvious that the calculated total absorbed dose rates for all waste samples are higher than the accepted dose levels. It is clear that the absorbed dose rates depend on the activities of g-emitters (e.g.  $^{226}\text{Ra}$ ,  $^{232}\text{Th}$ ,  $^{40}\text{K}$ ). Therefore, the total absorbed dose rate values increase with the activity concentration, and consequently enhances the radiological impact on the workers in the building material industries.

The absorbed dose rates in indoor air calculated from the measured activities in granite samples are also given in Table 4 (column 2) for the different granite types and the regions from where they were collected. The absorbed dose rates in indoor air were found to vary from  $74.60$  to  $237.69 \text{ nGy h}^{-1}$  with a mean value of  $150.53 \text{ nGy h}^{-1}$ . Average absorbed dose rates for all samples are higher than the world average value of  $55 \text{ nGy/h}$  [27]. Studies indicate an average outdoor terrestrial gamma dose rate of  $60 \text{ nGy/h}$  in the world ranging from  $10$  to  $200 \text{ nGy/h}$  [3]. From the present work we found that the average terrestrial gamma dose rate is  $150.53 \text{ nGy/h}$  which is higher than the world average.

### 2.3.2. The Annual Effective Dose Equivalent ( $D_{\text{eff}}$ )

The annual effective dose equivalent received by a member has been calculated from the absorbed dose rate by applying dose conversion factor of  $0.7 \text{ Sv/Gy}$  and the occupancy factor for outdoor and indoor as  $0.2(5/24)$  and  $0.8(19/24)$ , respectively [38] using the following equations:

$$D_{\text{eff}}(\text{Outdoor}) (\text{mSv/y}) = (\text{Absorbed dose}) \text{ nGy/h} \cdot 8760\text{h} \cdot 0.7 \text{ Sv/Gy} \cdot 0.2 \times 10^{-6}, \quad (4)$$

$$D_{\text{eff}}(\text{Indoor}) (\text{mSv/y}) = (\text{Absorbed dose}) \text{ nGy/h} \cdot 8760\text{h} \cdot 0.7 \text{ Sv/Gy} \cdot 0.8 \times 10^{-6}. \quad (5)$$

The calculated outdoor and indoor  $D_{\text{eff}}$  values are given in Table 4. The minimum, the maximum and the average values for outdoor are  $0.09 \text{ mSv/y}$ ,  $0.29 \text{ mSv/y}$  and  $0.18 \text{ mSv/y}$ , respectively and the corresponding indoor values are  $0.37 \text{ mSv/y}$ ,  $1.17 \text{ mSv/y}$  and  $0.74 \text{ mSv/y}$  respectively. Table 5 shows the absorbed dose rate D ( $\text{nGy h}^{-1}$ ) and the annual effective dose  $D_{\text{eff}}$  ( $\text{mSv y}^{-1}$ ) estimated for the examined granite samples. The annual effective dose limit was considered to be  $1 \text{ mSv}$ . It was concluded that the absorbed dose rates for people living in dwellings made of the examined granites would be higher than the absorbed dose rates for those living in dwellings made of building materials having the regular soil composition. All samples have  $^{40}\text{K}$  activity concentrations higher than the double those of the regular soil values, except sample G(9) with activity concentrations of  $353.08 \text{ Bq/Kg}$ . Moreover samples G(4), G(5) and G(6) have  $^{232}\text{Th}$ ,  $^{238}\text{U}$  and  $^{226}\text{Ra}$ , activity concentrations higher than double those of the regular soil concentrations. Finally Samples G(5) and G(6) gave annual effective dose higher than  $1 \text{ mSv/y}$ , which characterized by the highest activity concentrations for all the measured radionuclides.

Table 5. The Calculated Radium Equivalent  $Ra_{\text{eq}}$  (Bq/Kg), Gamma and Alpha Activity Indices ( $I_\gamma$ ,  $I_\alpha$ ), ELCR

ELCR·10 <sup>-3</sup>	$I_\alpha < 1$	$I_\gamma < 1$	$Ra_{\text{eq}}$ (Bq/Kg)	Sample
0.73	1.06±0.07	2.46±0.13	343.34±18.8	G(1)
0.58	0.84±0.10	2.22±0.16	304.51±23.8	G(2)
0.47	0.97±0.09	2.13±0.17	297.75±24.9	G(3)
0.84	1.20±0.11	2.93±0.20	407.47±29.7	G(4)
0.93	1.29±0.11	3.25±0.21	455.36±30.9	G(5)
1.02	1.34±0.15	3.24±0.26	453.39±38.1	G(6)
0.50	0.89±0.09	1.87±0.17	265.00±24.4	G(7)
0.51	0.75±0.10	2.06±0.19	278.90±27.7	G(8)
0.32	0.81±0.08	1.41±0.14	202.89±20.9	G(9)
0.71	0.97±0.10	2.71±0.20	369.20±28.7	G(10)
0.50	0.86±0.08	2.09±0.15	285.09±21.2	G(11)
0.65	1.00±0.09	2.40±0.18	332.99±26.3	Average

### 2.3.3. Radiological Hazard Indices (Hin-Hex)

The Gamma ray radiation hazard indices from radionuclides in granite samples have been calculated. Even though total activity concentration of radionuclides is calculated, it does not provide the exact indication about the total radiation hazards. Also these hazard indices are used to select the right materials.

Hazard Indices ( $H_{\text{ex}}$  and  $H_{\text{in}}$ ), represent the external and internal radiation hazards. These indices were calculated [39, 40]. As given in Table 4 according to the following criterion:

$$H_{\text{ex}} = (A_{\text{U}}/370 + A_{\text{Th}}/259 + A_{\text{K}}/4810) < 1, \quad (6)$$

$$H_{\text{in}} = (A_{\text{U}}/185 + A_{\text{Th}}/259 + A_{\text{K}}/4810) < 1, \quad (7)$$

where  $A_{\text{U}}$ ,  $A_{\text{Th}}$  and  $A_{\text{K}}$  are the mean activity concentrations of  $^{238}\text{U}$ ,  $^{232}\text{Th}$  and  $^{40}\text{K}$  in Bq/Kg respectively. The values of these indices must be less than unity in order to keep the radiation hazard insignificant. The maximum value of  $H_{\text{ex}}$  equal to unity corresponds to the upper limit of  $Ra_{\text{eq}}$  ( $370 \text{ Bq kg}^{-1}$ ). In addition to the external hazard, radon and its short-lived products are also hazardous to the respiratory organs. The internal exposure to radon and its daughter products is quantified by the internal hazard index ( $H_{\text{in}}$ ) which is given by the equation (7). The  $H_{\text{ex}}$  and an internal hazard index  $H_{\text{in}}$  which controls the internal exposure to radon ( $^{222}\text{Rn}$ ) and its daughter products are similarly determined.

The values of  $H_{\text{ex}}$  for the studied granite samples range from  $0.55$  to  $1.23$ , with an average value of  $0.9$ , are less than unity. While the values of  $H_{\text{in}}$  for the studied granite samples are higher than unity except for sample G(9) as its mean value is  $0.98$ , Table 4. Hence the annual effective dose due to radioactivity in the samples studied is less than  $1.5 \text{ mSv y}^{-1}$ . Indoor radon levels will probably increase with increasing concentrations of  $^{226}\text{Ra}$  (or uranium) in the soils (or in building materials).



## 2.4. Assessment of Radiation Hazard From Granite Samples

### 2.4.1. Radium equivalent activity ( $Ra_{eq}$ )

It is important to assess the gamma radiation hazards to persons associated with the used sand, limestone, shale and granite for building materials. To represent the activities due to  $^{226}\text{Ra}$ ,  $^{232}\text{Th}$  and  $^{40}\text{K}$  by a single quantity which takes into account the radiation hazards which may be caused a common index called the radium equivalent activity ( $Ra_{eq}$ ) in  $\text{Bqkg}^{-1}$  has been introduced, defined as:

$$Ra_{eq} = A_{Ra} + 1.43 A_{Th} + 0.077A_K, \quad (8)$$

where  $A_{Ra}$ ,  $A_{Th}$  and  $A_K$  are the activity concentrations of  $^{226}\text{Ra}$ ,  $^{232}\text{Th}$  and  $^{40}\text{K}$  in  $\text{Bqkg}^{-1}$ , respectively. While defining  $Ra_{eq}$ , it has been assumed that 1  $\text{Bq kg}^{-1}$  of  $^{226}\text{Ra}$ , 0.7  $\text{Bq kg}^{-1}$  of  $^{232}\text{Th}$  and 13  $\text{Bq kg}^{-1}$  of  $^{40}\text{K}$  produce the same gamma-ray dose [39, 41, 42].

The world average of  $Ra_{eq}$  in soils is 89  $\text{Bq kg}^{-1}$  [43]. As reference, the permissible dose limit for public which is recommended by ICRP (1991) [44] is 1.5  $\text{mSv y}^{-1}$  or equivalent to 370  $\text{Bq kg}^{-1}$ . The mean calculated  $Ra_{eq}$  values are shown in Table 5 for the different granite types and the regions from where they were collected. The minimum (202.89  $\text{Bq kg}^{-1}$ ) and the maximum (455.36  $\text{Bq kg}^{-1}$ ) values of  $Ra_{eq}$  were found in G(9) and G(5) granite types, respectively. The mean  $Ra_{eq}$  values of all the measured samples were almost lower than the limit value of 370  $\text{Bq kg}^{-1}$  recommended by the Organization for Economic Cooperation and Development.

### 2.4.2. Activity Indices {Gamma-index ( $I_\gamma$ ) and Alpha Index ( $I_\alpha$ ):}

A number of indices dealing with the assessment of the external and internal radiations originating from building materials and gamma concentration indexes have been proposed by several investigators [45–48]. In this study, the gamma-index was calculated as proposed by the European Commission (EC, 1999):

$$I_\gamma = A_{Ra}/150 + A_{Th}/100 + A_K/1500, \quad (9)$$

where  $A_{Ra}$ ,  $A_{Th}$  and  $A_K$  are the activity concentrations of  $^{226}\text{Ra}$ ,  $^{232}\text{Th}$  and  $^{40}\text{K}$  in  $\text{Bqkg}^{-1}$ , respectively. The mean values of  $I_\gamma$  calculated from the measured activity concentrations of  $^{226}\text{Ra}$ ,  $^{232}\text{Th}$  and  $^{40}\text{K}$  are presented in Table 5 for different granite types and the regions from where they were collected. The calculated values of  $I_\gamma$  for the studied samples varied in the range between 1.41–3.25 for granite types are higher than the critical value of unity. The mean calculated values of  $I_\gamma$  for the studied samples varied in the range between G(5)– G(9) for all types of granite which were higher than the critical value of unity.

$I_\gamma < 1$  corresponds to a dose creation of 1  $\text{mSv y}^{-1}$ , while  $I_\gamma < 0.5$  corresponds to 0.3  $\text{mSv y}^{-1}$ . The values of the activity index ( $I_\gamma$ ) are shown in the third column of Table 5. It is clear from Table 5 that the mean value of the activity index  $I_\gamma$  is 2.40, which is higher than the upper limit for  $I_\gamma$ .

In Table 5 are summarized the activity indices ( $I_\gamma$ ) based on the dose calculation using the standard room model. However, this is not realistic since granite rocks are usually used in small quantities on floors or exterior walls of buildings, tables and various decorations in living rooms. Since, only a small portion of the materials in a typical building is granite, [30] used a reinforced concrete living room of 6 m x 4 m x 3 m with 0.2 m thick wall and 0.02 m thick granite floor as a more reasonable model. The granite material in this construction was estimated to be

only 2.2 % of the total weight. Using their own equation which takes into account the number of different kinds of the building materials, their weight ratio, and the specific activities of  $^{238}\text{U}$ ,  $^{226}\text{Ra}$ ,  $^{232}\text{Th}$  and  $^{40}\text{K}$  in them, they found that the calculated activity index for their worst granite sample, based on the standard room model (No. 3, with activity index ( $I_g$ ) = 1.57, their Table 3), is  $I_g = 0.38$ , which is far below 1. They also found that if the activity of sample No. 3 increases 10 times i.e ( $I_g = 15.7$ ), the corresponding activity index will be only  $I_g = 0.62$ . The highest  $I_g$ -value of our investigated samples (based on the standard room model) is 3.24 {G(6), Table 5}, far below 15.7, which corresponding to an  $I_g < 0.62$ . From the above calculations, granites used in Egypt as building materials would not induce an activity level exceeding the 1  $\text{mSv y}^{-1}$  dose limit.

So far, several alpha indices have been proposed to assess the exposure level due to radon inhalation originating from building materials [8]. The alpha index was determined using the following formula:

$$I_a = A_{Ra}/200 \text{ (Bq kg}^{-1}\text{)}, \quad (10)$$

where  $A_{Ra}$  ( $\text{Bq kg}^{-1}$ ) is the activity concentration of  $^{226}\text{Ra}$  assumed in equilibrium with  $^{238}\text{U}$ . The recommended exemption and upper level of  $^{226}\text{Ra}$  activity concentrations in building materials are 100 and 200  $\text{Bq kg}^{-1}$ , respectively, as suggested by [49]. These considerations are reflected in the alpha index. The recommended upper limit concentration of  $^{226}\text{Ra}$  is 200  $\text{Bq kg}^{-1}$ , for which  $I_a = 1$ .

The mean computed  $I_a$  values for the studied samples are given in Table 5 for the different granite types and the regions where they were collected. The values of  $I_a$  ranged from (0.75 to 1.34), with the mean value of 1.00. For the safe use of a material in the construction of dwellings,  $I_a$  should be less than unity. The mean calculated values were equal unity.

### 2.4.3. Excess Lifetime Cancer Risk (ELCR)

Excess Lifetime Cancer Risk (ELCR) has been calculated using the equation below and is shown in Table 5.

$$\text{ELCR} = D_{\text{eff}} \times \text{DL} \times \text{RF}, \quad (11)$$

where  $D_{\text{eff}}$ , DL and RF are the annual effective dose equivalent, the duration of life (70 years) and the risk factor ( $\text{Sv}^{-1}$ ), fatal cancer risk per sievert. For stochastic effects, [44] uses values of 0.05 for the public [3]. The range of ELCR is  $0.32 \times 10^{-3}$  to  $1.02 \times 10^{-3}$  with an average of  $0.65 \times 10^{-3}$ . Average ELCR for all samples is higher than the world average ( $0.29 \times 10^{-3}$ ). Which means that all samples have higher ELCR value.

## Conclusions

The activities of the natural radionuclides  $^{238}\text{U}$ ,  $^{226}\text{Ra}$ ,  $^{232}\text{Th}$  and  $^{40}\text{K}$  in the granite samples collected from suppliers, grinding plants and factories in Egypt were measured by using the technique of gamma-ray spectroscopy with HPGe detector. The results may be useful in the assessment of the exposures and the radiation doses due to the natural radioactive element contents in granite sample. Analysis was carried out to examine its impact on human health and the environment.

The activity concentrations of  $^{238}\text{U}$ ,  $^{226}\text{Ra}$ ,  $^{232}\text{Th}$  and  $^{40}\text{K}$  of most of the granites exceed the average level of these



radionuclides in regular soil  $35 \text{ Bq} \cdot \text{kg}^{-1}$ ,  $35 \text{ Bq} \cdot \text{kg}^{-1}$ ,  $30 \text{ Bq} \cdot \text{kg}^{-1}$  and  $400 \text{ Bq} \cdot \text{kg}^{-1}$ , respectively. The corresponding absorbed dose rate from all those radionuclides also exceeds significantly the average value of  $55 \text{ nGy} \cdot \text{h}^{-1}$  from these terrestrial radionuclides in regular soil. Although the annual effective dose is higher than the limit of  $1 \text{ mSv} \cdot \text{y}^{-1}$  for some studied granites, in particular the samples G(4), G(5) and G(6), they could be used safely as building materials, considering that their contribution in most of the house constructions is very low, as we suggest in section 3.3.2.

The high level of natural radioactivity of the investigated granites is connected with the presence of both the K-rich minerals (K-feldspars, biotite) and accessories (monazite, zircon, apatite, titanite, allanite and hematite) which are mainly found in granitic rocks. This justifies the low level of radioactivity of the sample G(9), deviating from the granitic composition, which means that they do not contain K-rich minerals and the above accessories. Obtained values show that the mean radium equivalent activities ( $R_{\text{eq}}$ ), gamma indices ( $I_{\text{g}}$ ), alpha indices ( $I_{\text{a}}$ ), the indoor absorbed dose rate (D) and the annual effective dose rate ( $D_{\text{eff}}$ ) outdoor – indoor, in granite samples are  $332.99 \text{ Bq} \cdot \text{kg}^{-1}$ , 2.4, 1.00,  $150.53 \text{ nGy} \cdot \text{h}^{-1}$  and  $(0.18-0.74) \text{ mSv} \cdot \text{y}^{-1}$ , respectively. The results show that the activity concentrations were not within the acceptable limits and the use of granite in the construction of buildings may be rise to any significant radiation exposure to the occupants.

Large variation among the radioactivity concentration for different sites has been observed, which might be a source for granite used for cladding and decoration of buildings in cities. It may be due to geological condition. The highest concentration was observed in Aswan city and Red sea area, the samples G(4), G(5) and G(6). The present study has pointed out the enhanced activity areas under investigation need further studies in order to better understand the presence of high dose rate. Any changes or increased to the dose rates in future we can deduce that contamination have taken place. The data can be used as a base line for preparing a radiological map of Egypt.

## References

1. J. A.K.V. Malathi, A. Andal, R. Paramesvaran, Vijayshankar and S. Selvasekarapandian, 'Study of indoor gamma radiation in Coimbatore City, Tamilnadu, India', International Congress Series 1276 (2005), pp. 344–345.
2. UNSCEAR, 1993, Sources and Effects of Ionizing Radiation. Report to General Assembly with Scientific Annexes, United Nations, New York.
3. H. Taskin, M. Karavus, P. Ay, A. Topuzoglu, S. Hindiroglu and G. Karahan, 2009, Radionuclide concentrations in soil and lifetime cancer risk due to the gamma radioactivity in Kirklareli, Turkey. Journal of Environmental Radioactivity, 100: 49–53.
4. M. Tzortzis, H. Tsertos, S. Christofides, G. Christodoulides, 2003. Gamma radiation measurements and dose rates in commercially-used natural tiling rocks (granites). J. Environ. Radioact. 70, 223–235.
5. V. Ramasamy, V. Ponnusamy and V. Gajendran, 2005, Evaluation of natural radioactivity and radiological hazards in various granites of Tamilnadu. Indian J. of Physics., 79(11): 1293–1297.
6. G. Faure, Chapter 18: the U, Th–Pb methods of dating. Principles of isotope geology, 2nd. New York7 John Wiley and Sons Inc.; 1986. p. 228–308.
7. F. Bea, Uranium. In: Marshall CP, Fairbridge RW, editors. Encyclopedia of geochemistry. Dordrecht7 Kluwer Academic Publisher; 1999. p. 645–648.
8. European Commission (EC), Radiation Protection 112. Radiological Protection Principles Concerning the Natural Radioactivity of Building Materials, Directorate-General Environment, Nuclear Safety and Civil Protection, 1999.
9. M. Ivanovich, Harmon RS, eds. Uranium Series Disequilibrium: Applications to Earth, Marine and Environmental Sciences. Oxford: Clarendon (1992). J. Phys. 25 (2), 133–144.
10. P. Elles, S. Y. Lee, Radionuclide-contaminated soil: a mineralogical perspective for their remediation. In: Dixon JB, Schulze DG, editors. Soil mineralogy with environmental applications. Madison, Wisconsin7 Soil Sci Soc of America; 2002. p. 737–63. [Chapter 25].
11. M. T. Me'nager, Heath, M. J., Ivanovich, M., Montjotin, C., Barillon, C. R., Camp, J., Hasler, S. E., 1993. Migration of uranium from uranium-mineralised fractures into the rock matrix in granite: implications for radionuclide transport around a radioactive waste repository. Fourth International Conference of Chemistry and Migration Behaviour of Actinides and Fission Products in the Geosphere (Migration, 1993), Charleston, USA, 12–17, December 1993, Radiochimica Acta 66/67, 47–83.
12. J.J.W. Rogers, P.C. Ragland, 1961. Variation of thorium and uranium in selected granitic rocks. Geochim. Cosmochim. Acta 25, 99–109.
13. MMRO, 2002. Projeto Multimim—MMRO—Ornamental Stones.
14. D. Amrani, M. Tahtat, 2001, Natural radioactivity in Algerian building materials. Appl. Radiat. Isot. 5(4) 687–689.
15. K. Khan, M. Aslam, S. D. Orfi, H.M.han, 2002, Norm and associated radiation hazards in bricks fabricated in various locations of the North-west Frontier (Pakistan). J. Environ. Radioact. 58(1) 59–66
16. K. Komura, 1997, Challenge to detection limit of environmental radioactivity. Proceedings of the 1997 International Symposium on Environmental Radiation, Tsuruga, Fukui, Japan, October 20, pp. 56–75.
17. K. Komura, A. M. Yousef, 2000, Natural radionuclides induced by environmental neutrons. Proceedings of the International Workshop on Distribution and Speciation of Radionuclides in the Environment, Rokkasho, Aomori, Japan. October 11–13, pp. 210–217.
18. C. A. Papachristodoulou, P. A. Assimakopoulos, N. E. Patronis, K. G. Loannides, 2003. Use of HPGe gray spectrometry to assess the isotopic composition of uranium in soils. Journal of Environmental Radioactivity 64 (2–3), 195–203.
19. R. M. Keyser, 1995, Characterization and Applicability of Low-Background Germanium Detectors, Technical Note, EG&G ORTEC, Oak Ridge, TN, USA.
20. P. Hayumbu, M. B. Zaman, N.C.H. Lubaba, S. S. Munsanje, and D. Nuleya, J. Radioanal. Nucl. Chem. 199, pp. 229–238, 1995.
21. N. Lavi, F. Groppi, Z.B. Alfassi, 2004. On the measurement of  $^{40}\text{K}$  in natural and synthetic materials by the method of high-resolution gamma ray spectrometry. Radiat. Meas. 38, 139–143.
22. V. J. Smith, L. W. Brown, 1988. Feldspar minerals. 1. Crystal structures, physical, chemical and microtextural properties. Springer-Verlag, Berlin, Heidelberg, New York, London, Paris, Tokyo.
23. W.M.E. Heinrich, 1958. Mineralogy and geology of radioactive raw materials. McGraw-Hill Book Company, New York.
24. M. Krmar, J. Slivka, E. Varga, I. Bikit and M. Veskovc, 2009. Correlations of natural radionuclides in sediment from Danube. J. of Geochemical Exploration., 100(1): 20–24.
25. B. A. Powell, L. D. Hughes, M. A. Sorefan, Deborah Falta, Michael Wall and T. A. Devol, 2007. Elevated concentrations of primordial radionuclides in sediments from the Reedy river and surrounding creeks in Simpsonville, South Carolina. J. of Environmental Radioactivity., 94: 121–128.
26. Y. Orgun, N. Altınsoy, A. H. Gultekin, G. Karahan, N. Celebi, 2005. Natural radioactivity levels in granitic plutons and groundwaters in Southeast part of Eskisehir, Turkey. Appl. Radiat. Isot. 63, 267–275.
27. UNSCEAR, 2000, Sources and Effects of Ionizing Radiation. Report to General Assembly, with Scientific Annexes, United Nations, New York
28. D. Malczewki, L. Taper, J. Dorda, 2004, Assessment of natural and anthropogenic radioactivity levels in rocks and soils in the environs of Swieradow Zdroj in Sudetes, Poland by in situ gamma – ray spectroscopy. J. Environ. Radioact. 73, 233–245.
29. Y. S. Krbish, I. O. Abugassa, N. Benfaid, A. A. Bashir, Instrumental neutron activation analysis for the elemental analysis of cement, J. Radioanal. Nucl. Chem. 271(2007) 63–69.

30. C. J. Chen, Y. M. Lin, 1996. Assessment of building materials for compliance with regulations of ROC. *Environment International*.
31. A. M. El-Arabi, 2005. Gamma activity in some environmental samples in South Egypt. *Indian J. Pure Appl. Phys.* 43, 422–426.
32. R. Anjos, E. Okuno, P. Gomes, R. Veiga, L. Estellita, L. Mangia, D. Uzka, T. Soares, A. Facure, J. Brage, B. Mosquera, C. Carvalho, A. Santos, 2004. Radioecology teaching: evaluation of the background radiation levels from areas with high concentrations of radionuclides in soil. *Eur.*
33. N. K. Ahmed, A. Abbady, A. M. El Arabi, R. Michel, A. H. El-Kamel, A. G. Abbady, 2006. Comparative study on the natural radioactivity of some selected rocks from Egypt and Germany. *Indian J. Pure Appl. Phys.* 44, 209–215.
34. K. N. Yu, Z. J. Guan, Z. J. Stocks, E. C. M. Young, 1992. The assessment of the natural radiation dose committed to the Hong Kong people. *J. Environ. Radioact.* 17, 31–48.
35. D. C. Kocher and A. L. Sjoreen, 1985. Dose-rate conversion factors for external exposure to photon emitters in soil. *Health Physics* 48: 193–205.
36. P. Jacob, H. G. Paretzke, H. Rosenbaum, M. Zanki, 1986. Effective dose equivalents for photon exposure from plane sources on the ground. *Radiat. Prot. Dosim.* 14: 299–310.
37. K. C. Leung, S. Y. Lau, C. B. Poon, 1990. Gamma radiation dose from radionuclides in Hong Kong soil. *J. Environ. Radioactive* 11: 279–290.
38. R. G. Veiga, N. Sanches, R. M. Anjos, K. Macario, J. Bastos, M. Iguatemy, J. G. Aguiar, A. M. A. Santos, B. Mosquera, C. Carvalho, M. Baptista Filho and N. K. Umisedo, 2006. Measurement of natural radioactivity in Brazilian beach sands. *Radiation measurements.*, 41: 189–196.
39. J. Beretka, P. J. Mathew, Natural radioactivity of Australian building materials, industrial wastes and by-products, *Health Phys.* 48 (1985) 87–95.
40. Y. Orgun, N. Altinsoy, S. Y. Sahin, Y. Gungor, A. H. Gultekin, G. Karaham and Z. Karaak, 2007. Natural and anthropogenic radionuclides in rocks and beach sands from Ezine region (canakkale), Western Anatolia, Turkey. *Applied Radiation and Isotopes.*, 739–747: 65.
41. A. Malanca, V. Passina, G. Dallara, 1993. Radionuclide content of building materials and gamma ray dose rates in dwellings of Rio Grande Do Norte, Brazil. *Radiat. Prot. Dosim.* 48, 199.
42. M. Iqbal, M. Tufail, S. M. Mirza, 2000. Measurement of natural radioactivity in marble found in Pakistan using a NaI(Tl) gamma-ray spectrometer. *J. Environ. Radioact.* 51, 255–256.
43. UNSCEAR. 1988, United Nations Scientific Committee on the Effects of Atomic Radiation. Sources Effects and Risk of Ionizing Radiation United Nations, New York.
44. ICRP, Annals of the ICRP, 1990, Recommendations of the International Commission on Radiological Protection, ICRP Publication 60, Oxford: Pergamon Press, 1991.
45. V. R. Krieger, 1981. Radioactivity of construction materials. *Betonwerk Fertigteil Tech.* 47, 468–473.
46. E. M. Kriuk, S. I. Tarasov, V. P. Shamov, N. I. Shalak, E. P. Lisachenko, L. G. Gomelsky, 1971. A Study on Radioactivity in Building Materials. Research Institute for Radiation Hygiene, Leningrad.
47. E. Stranden, 1976. Some aspects on radioactivity of building materials. *Physica Norvegica* 8, 167–173.
48. M. Markkanen, 1995. Radiation dose assessments for materials with elevated natural radioactivity. Report STUK-B-STO 32, Radiation and Nuclear Safety Authority e STUK.
49. ICRP, Protection against Rn-222 at home and at work. Publication No. 65; *Ann. ICRP* 23 (2), Pergamon, Oxford, 1994.

Received 22.12.2011.